Geol. Mag. **151** (*2*), *2014, pp. 201–215.* © *Cambridge University Press 2013*
doi:10.1017/S0016756812001057

A high-resolution, multiproxy stratigraphic analysis of the Devonian–Carboniferous boundary sections in the Moravian Karst (Czech Republic) and a correlation with the Carnic Alps (Austria)

TOMÁŠ KUMPAN*†, ONDŘEJ BÁBEK*‡, JIŘÍ KALVODA*, JIŘÍ FRÝDA§¶ & TOMÁŠ MATYS GRYGAR‖

*Department of Geological Sciences, Masaryk University, Kotlářská 2, 611 37, Brno, Czech Republic
‡Department of Geology, Palacký University, 17. listopadu 12, 772 00, Olomouc, Czech Republic
§Institute of Inorganic Chemistry AS CR, v.v.i., 250 68, Řež, Czech Republic
¶Czech Geological Survey, Klárov 3/131, 118 21, Prague 1, Czech Republic
‖Department of Environmental Geosciences, Czech University of Life Sciences, Kamýcká 129, 165 21, Prague 6, Czech Republic

(*Received* 2 July 2012; *accepted* 7 December 2012; *first published online* 2 May 2013)

Abstract – A multidisciplinary correlation of the Devonian–Carboniferous (D–C) boundary sections from the Moravian Karst (Czech Republic) and the Carnic Alps (Austria), based on conodont and foraminifer biostratigraphy, microfacies analysis, field gamma-ray spectroscopy (GRS), carbon isotopes and element geochemistry, is presented in this paper. The study is focused on the interval from the Middle *Palmatolepis gracilis expansa* Zone (Late Famennian) to the *Siphonodella sandbergi* Zone (Early Tournaisian). In Lesní lom (Moravian Karst), a positive $\delta^{13}C$ excursion in the *Bisphatodus costatus – Protognathodus kockeli* Interregnum from a distinct laminated carbonate horizon is correlated with a carbon isotope excursion from the Grüne Schneid section of the Carnic Alps and is interpreted as the equivalent of the Hangenberg black shales and a local expression of the global Hangenberg Event *sensu stricto*. Higher up at both sections, a significant increase in the terrigenous input, which is inferred from the GRS signal and elevated concentrations of terrigenous elements (Si, Ti, Zr, Rb, Al, etc.), provides another correlation tieline and is interpreted as the equivalent of the Hangenberg sandstone. Both horizons are discussed in terms of relative sea-level fluctuations and palaeoceanographic changes. Recent studies show that conodont biostratigraphy is facing serious problems associated with the taxonomy of the first siphonodellids, their dependence on facies and discontinuous occurrences of protognathodids at the D–C boundary. Therefore, the correlative potential of geochemical and petrophysical signatures is high and offers an alternative for the refining of the problematic biostratigraphic division of the D–C boundary.

Keywords: Hangenberg Event, gamma-ray spectra, carbon isotopes, element geochemistry.

1. Introduction

The Devonian–Carboniferous (D–C) boundary represents a prominent time interval that is associated with global eustatic perturbations, glaciation in Gondwana, palaeoceanographic changes, global biotic extinction and faunal overturns (Walliser, 1984; Caputo & Crowell, 1985; Isaacson *et al*. 2008). In numerous sections, the D–C successions are manifested by distinct facies such as the well-documented Hangenberg black shales (HBS) and Hangenberg shales and sandstone (HSS); the former is assumed to indicate a biotic event (the Hangenberg Event *sensu stricto*) of global importance (Walliser, 1984). In spite of the correlative value of these latest Devonian and earliest Carboniferous events, the chronostratigraphic definition of the D–C boundary (GSSP) is based purely on biostratigraphic constraints, i.e. the first appearance datum (FAD) of the *Siphonodella sulcata* conodont in the early evolutionary lineage of the genus *Siphonodella* (Flajs & Feist, 1988). New data from the D–C stratotype in the GSSP at La Serre, southern France, reveal that the first occurrence of the index fossil *Si. sulcata* is located much lower in the stratigraphic succession than previously reported and that the La Serre D–C boundary GSSP requires re-positioning (Kaiser, 2009). The limestone beds in La Serre only contain rare *Siphonodella* and reveal a diachronous occurrence of *Si. sulcata*, which is often controlled by facies (Ziegler & Sandberg, 1984). The new findings of *Si. sulcata* draw the position of the D–C boundary closer to the global Hangenberg Event, which is regarded by Walliser (1984) as a worldwide synchronous, natural D–C boundary. The glacioeustatic nature of the Hangenberg Event was proposed by Kalvoda (1986) and later confirmed by the discovery of glacial sediments in the South American part of Gondwana (Isaacson *et al*. 1999, 2008; Streel *et al*. 2000). In many European sections (Carnic Alps, Rheinsche Schiefergebirge, Montagne Noire), the Hangenberg Event is associated with a positive carbon isotope excursion, which is interpreted as a result of increased

†Author for correspondence: kumpan.tom@gmail.com

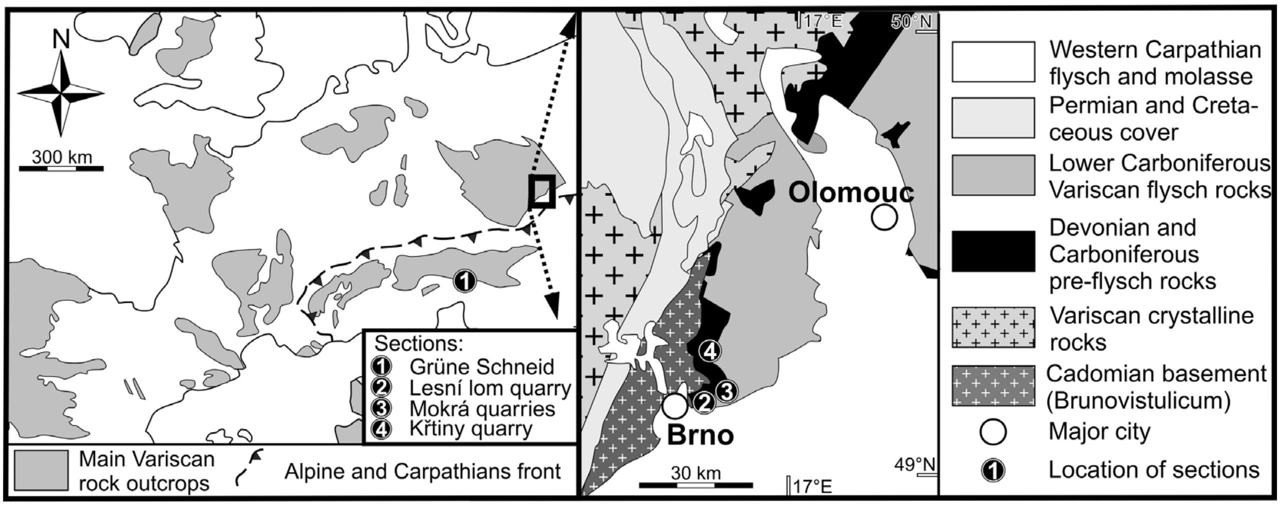

Figure 1. Location of the studied sections.

burial of organic matter in the global ocean (Buggisch & Joachimski, 2006; Kaiser *et al.* 2006; Kaiser, Steuber & Becker, 2008). The stable isotope geochemistry can therefore provide a reasonable solution to the event-based D–C boundary.

Both biostratigraphy and isotope geochemistry, however, have their well-known limits; the latter being expensive, instrumentally demanding and susceptible to compositional bias, particularly in the Palaeozoic (Veizer, 2009). In addition, a significant gap may occur between discrete and fragmentary representations of the isotope curves and the vertical continuum of a real stratigraphic column. An alternative approach can be found in proxy parameters such as the gamma-ray spectrometry (GRS) of carbonate rocks (Rider, 1999; Ehrenberg & Svana, 2001; Halgedahl *et al.* 2009; Koptíková *et al.* 2010) – a method which is inexpensive, quantitative and applicable directly in the field. GRS can quickly provide high-quality, high-resolution proxy data, which can be interpreted in terms of a siliciclastic admixture in carbonates, redox conditions at the sediment–water interface and, hence, relative sea-level changes (Postma & Ten Veen, 1999; Lüning *et al.* 2004; Bábek *et al.* 2010). In addition, the petrophysics and isotope geochemistry data can be significantly enhanced by element geochemistry to provide a multiproxy geochemical mosaic, which can be used for correlation purposes and for the interpretation of the steering mechanisms on deposition (terrigenous input, redox conditions, bioproductivity).

In this paper, we combined conodont and foraminifer biostratigraphy with carbonate compositional analysis, GRS, carbon isotopes and major- and trace element geochemistry at three D–C sections in the Moravian Karst, SE Czech Republic (Fig. 1). At these sections, the FAD of *Si. sulcata* can be well traced in different deep-water carbonate facies (Kalvoda & Kukal, 1987; Kalvoda, Bábek & Malovaná, 1999; Kalvoda, 2002) (Fig. 2). The co-occurrence of shallow-water foraminifers and deep-water conodonts in cal-

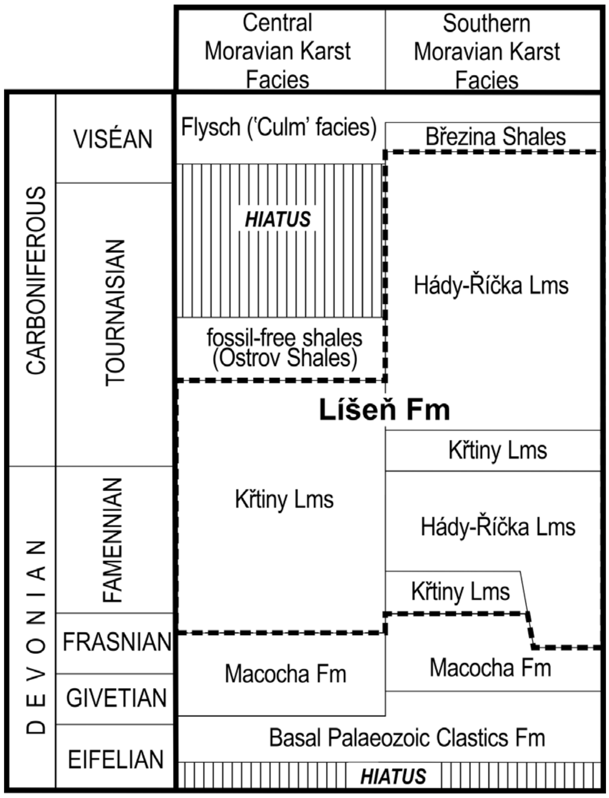

Figure 2. Generalized lithostratigraphy of the central and southern part of the Moravian Karst (after Kalvoda *et al.* 2008).

citurbidite facies enables a good correlation between the conodont-based zonations and the foraminifer zonations of the East European platform and the Urals. The Moravian Karst sections (southern Laurussia) are correlated with the Carnic Alps (Intra-Alpine, peri-Gondwana terrane), based on the published isotope data (Kaiser *et al.* 2006) and our new GRS and element geochemistry data from the well-known Grüne Schneid section. The aim of the paper is to present the quantitative multiproxy method as a useful correlative tool in the event-based solution of the D–C boundary and to advocate its benefits in Palaeozoic stratigraphy.

https://doi.org/10.1017/S0016756812001057 Published online by Cambridge University Press

2. Geological setting and stratigraphy

The studied sections Lesní lom Quarry (WGS 84: 49° 13′ 19.78″ N; 16° 41′ 49.73″ E), Mokrá Quarry (WGS 84: 49° 13′ 43.94″ N; 16° 46′ 8.40″ E) and Křtiny Quarry (WGS 84: 49°17′ 38.10″ N, 16° 44′ 9.76″ E) are located NE of Brno in the southern and central parts of the Moravian Karst, Moravia, Czech Republic (Fig. 1). The Middle Devonian to Viséan carbonates (Macocha and Líšeň formations) of the Moravian Karst (Figs 1, 2) represent the sedimentary cover of the Brunovistulian terrane, which is generally regarded as an eastern continuation of the Rhenohercynian Zone at the southern margin of Laurussia (Kalvoda,1998; Kalvoda *et al*. 2002, 2003, 2008).

On top of the drowned platforms of the Macocha Fm (Hladil, 1994) and in the troughs, condensed hemipelagites and calciturbidites (Líšeň Fm) were deposited in the Late Frasnian to early Viséan period (Kalvoda, Bábek & Malovaná, 1999). Facies development of the Líšeň Fm (Fig. 2) in the southern part of the Moravian Karst (Lesní lom and Mokrá) comprises largely skeletal calciturbidites in the Famennian (Hády-Říčka Lms), mud calciturbidites (Křtiny Lms) in the Early Tournaisian and skeletal calciturbidites (Hády-Říčka Lms) from the Middle Tournaisian to the early Viséan. In the central part of the Moravian Karst (Křtiny), nodular hemipelagic Křtiny Lms range from the Famennian to the Early Tournaisian. An onlap of deep-water shales, radiolarian cherts and siliciclastic turbidites of 'Culm' flysh facies on the Líšeň Fm takes place in the early Viséan (Kalvoda, Bábek & Malovaná, 1999).

3. Material and methods

The lithology of the sections was logged in a bed-by-bed manner. The sections were sampled in great detail for conodont and foraminifer biostratigraphy, quantitative microfacies analysis, element geochemistry and carbon isotope geochemistry.

Samples for conodonts (2–4 kg each) were taken from each limestone bed and then dissolved in 15 % acetic acid. Conodonts were hand-picked from the sieved (mesh size 0.125) insoluble residues and then studied under a binocular microscope. Foraminifers were studied in a large number (about 200 thin-sections) of standard size (27 × 46 mm) thin-sections with a high-magnification binocular microscope (Nikon 80i) in transmitted light at magnifications ranging from × 20 to × 400.

The quantitative microfacies analysis was focused on compositional variations of major allochem groups in 60 carbonate samples from the Lesní lom section. Qualitative microscopic observations were followed by point counting of high-resolution images (250 random points per image) using JMicroVision image analysis software (Nicolas Roduit, Switzerland).

The lithological description and sampling was supported by field GRS logging, using a RS-230 Super Spec portable spectrometer (Radiation Solutions, Inc., Canada) with a 2 × 2′ (103 cm^3) bismuth-germanate (BGO) scintillation detector. The measurement at each logging point was performed on a flat rock surface (2π geometry), perpendicular to the section wall and with the instrument in full contact with the rock (Svendsen & Hartley, 2001, p. 662). One measurement with a 180 s count time was performed at each logging point. The sections were logged with a 0.25 m thickness interval and 223 GRS data points were measured. The time-dependent measurements revealed that the concentrations of K, U and Th sufficiently stabilized after 120 to 150 s. The counts per second in selected energy windows were converted to concentrations of K (%), U (ppm) and Th (ppm) automatically by the instrument, based on calibrations carried out by the manufacturer on test pads with a known elemental composition. Computed gamma-ray (CGR) values, used as improved clay volume indicators, were calculated from the spectral values using the formula CGR [API] = Th[ppm]·3.93 + K[%]·16.32 (Rider, 1999).

For carbon isotope geochemistry, several milligrams of rock powder (preferably micrite from lime mudstone and wackestone lithologies) were recovered from rock fragments. The carbonate powder was reacted with phosphoric acid in an online carbonate preparation system (Carbo-Kiel) connected to a ThermoFinnigan 252 mass spectrometer. All the values are reported in ‰ relative to V-PDB (Vienna Pee-Dee Belemnite) by assigning a $\delta^{13}C$ value of +1.95 ‰ and a $\delta^{18}O$ value of 2.20 ‰ to NSB 19. The accuracy and precision were controlled by replicate measurements of laboratory standards and were better than ± 0.1 ‰ for both carbon and oxygen isotopes.

Element analyses were performed by energy dispersive X-ray fluorescence spectrometry (XRF) using MiniPal 4.0 (PANalytical, the Netherlands) with a Rh lamp and Peltier cooled Si PIN detector. Hand-ground samples were poured into plastic cells with Mylar foil bottoms with a diameter of 25 mm. Al and Si signals were acquired for 300 s at 5 kV/400 μA with a Kapton filter under He flush (99.996 % purity), K, Ti, Fe, and Mn and Fe for 200 s at 12 kV/200 μA with a thin Al filter in air, and Zr for 500 s at 30 kV/200 μA with a Ag filter in air. The XRF proxy signal was calibrated by analyses of 11 samples by an accredited analytical laboratory in TU Ostrava, Czech Republic. The samples were finely powdered in a ball mill, pressed with a Hoechst Wachs C Mikropulver and analysed with an XRF spectrometer SPECTRO X-LAB (3 kW Rh-tube, liquid nitrogen cooled Si (Li) detector).

4. Results

4.a. Biostratigraphy

The latest Famennian and Early Tournaisian conodont zonation *sensu* Ji (1985) and Kaiser *et al*. (2009) is used in this paper and is presented with the former standard conodont zonations (Sandberg *et al*. 1978; Ziegler &

https://doi.org/10.1017/S0016756812001057 Published online by Cambridge University Press

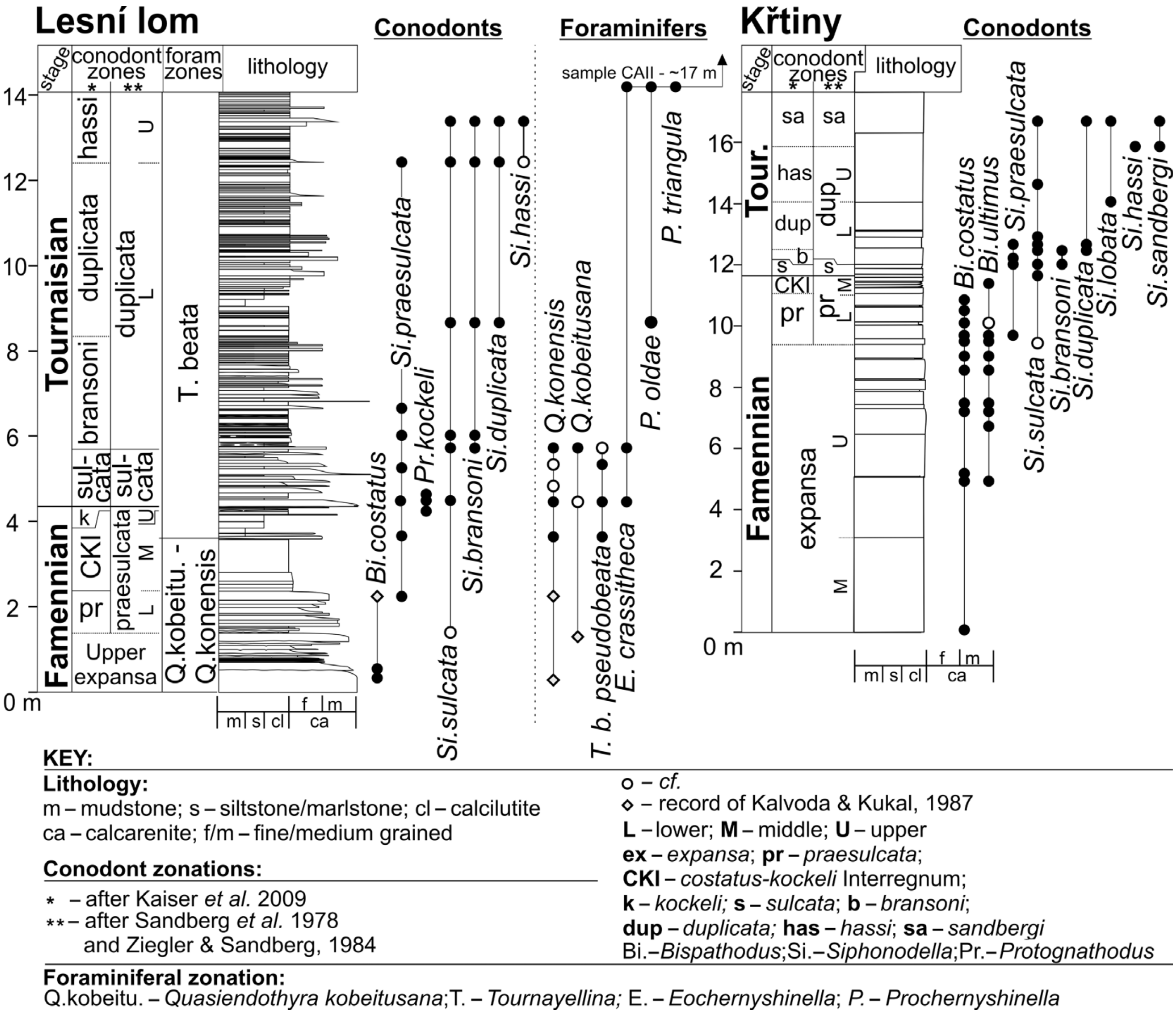

Figure 3. Lithology and distribution of the most important conodonts and foraminifers in the Lesní lom and Křtiny Quarry sections.

Sandberg, 1984) and foraminiferal zonation (Kalvoda, 2002) in Figure 3.

The studied D–C boundary interval begins in the Middle *Palmatolepis gracilis expansa* Zone in Křtiny and in the Upper *expansa* Zone in Lesní lom and most probably Mokrá (Fig. 3). The base of the *Siphonodella praesulcata* Zone is difficult to locate owing to the scarcity of the early siphonodellids and the similarity of the associated conodont fauna with the underlying Upper *expansa* Zone. The first siphonodellids from Lesní lom (unpublished specimen from the collection of Dr Krejčí, Czech Geological Survey, Brno) and Křtiny rank among the morphotypes of *Si. sulcata* (Group 1 *sensu* Kaiser & Corradini, 2011), whereas the first typical *Si. praesulcata* (Groups 2 and 3 *sensu* Kaiser & Corradini, 2011) occurs higher within the *praesulcata* Zone. Both in Lesní lom and Mokrá, the conodont-sterile laminite, assigned to the *Bispathodus costatus – Protognathodus kockeli* Interregnum (CKI), is overlain by an interval of silty marlstones with scarce limestone nodules. The nodules yielded, in Lesní lom, relatively abundant *Pr. meischneri* and *Pr. collinsoni* at the base, and the first specimens of *Pr. kockeli* at the top of this interval. Because of the absence of protognathodids, there is no biostratigraphic evidence of the *kockeli* Zone in Křtiny. The *sulcata* Zone with relatively abundant *Si. sulcata*, *Pr. kuehni* and reworked Late Famennian conodonts (Bábek & Kalvoda, 2001) was distinguished in Lesní lom (Fig. 3) and at the tectonically disturbed Mokrá–Central Quarry section at the base of ooidal-bioclastic calciturbidites. The abrupt onset of the relatively abundant *Si. sulcata* and transition morphotypes close to *Si. bransoni* just above the D–C boundary in Křtiny points to a hiatus in the lower parts of the *sulcata* Zone. The overlying *Siphonodella bransoni*, *Siphonodella duplicata* and *Siphonodella hassi* zones are well marked by their index and accompanying taxa in the Lesní lom and Křtiny quarries. The uppermost part of the investigated section in Křtiny contains an association of the *Siphonodella sandbergi* Zone (Fig. 3).

Foraminifers of the middle Palaeozoic were benthic and only associated with a shallow-water environment (Vachard, Pille & Gaillot, 2010). Their presence in the

Lesní lom section is tied to the bioclastic calciturbidites (Kalvoda, Bábek & Malovaná, 1999). The studied section in Lesní lom (Fig. 3) begins below the laminite in the Upper Famennian *Quasiendothyra kobeitusana* – *Q. konensis* Zone (Kalvoda & Kukal, 1987). The *Tournayellina beata* Zone associated with the entry of its index species *Tournayellina beata pseudobeata* (Barskov *et al*. 1984; Kalvoda & Kukal, 1987; Reitlinger & Kulagina, 1987; Kalvoda, 2002; Kulagina, Gibshman & Pazukhin, 2003; Pazukhin, Kulagina & Sedaeva, 2009) is recognized just above the laminite in the CKI (Fig. 3). In contrast to the Belgian sections (Poty, Devuyst & Hance, 2006), the *Tournayellina beata* Zone is also characterized by the presence of quasiendothyrs, which continue well into the Tournaisian *bransoni* Zone. Quasiendothyrids are not associated with intraclasts and there are no differences in their preservation in comparison with Tournaisian chernyshinellids. Consequently, their reworking from Upper Famennian limestones seems to be highly improbable. Moreover, the obtained associations resemble those in the Urals where quasiendothyrids (*Quasiendothyra communis*. *Quasiendothyra* sp., *Quasiendothyra* ex gr. *konensis*) are also reported in the earliest Tournaisian (Reitlinger & Kulagina, 1987; Pazukhin, Kulagina & Sedaeva, 2009). The rare occurrence of chernyshinellids, represented by *Eochernyshinella crassitheca*, *Prochernyshinella oldae* and at the very top of the section also *Prochernyshinella triangula*, is typical in the Tournaisian part of the section (Fig. 3).

4.b. Facies and microfacies characteristics

Five facies types with seven microfacies subtypes (Table 1) were distinguished in the measured sections, based on the bedding patterns, grain size, sedimentary structures and allochem composition. All facies types were deposited in relatively deep water, well below the fair-weather wave base, as indicated by abundant radiolarians, sponge spicules, thin-shelled bivalves, trilobites and the ubiquitous presence of lime mud in the autochthonous deposits. Their deep-water origin is supported by abundant conodonts of the palmatolepid-bispathodid and siphonodellid biofacies. Nodular, micrite-rich facies with abundant pelagic faunas (F5) are interpreted to represent suspension deposits, analogous to the recent periplatform oozes (Boardman & Neumann, 1984) and Palaeozoic 'pelagic' deposits (Bandel, 1974). Considerable parts of the sedimentary record (Lesní lom and Mokrá sections) comprise thin-bedded calcarenites and calcisiltites (F4) with frequent erosive bed bases, graded bedding, bed-parallel lamination and mixed shallow-water benthic (ooids, peloids, foraminifers, dasyclad algae, echinoderms) and pelagic and deep-water (radiolarians, sponge spicules) allochems, often with biogenic grading. This facies is interpreted as relatively medium to distal carbonate turbidites. These facies alternate with marly and shaly background interbeds (F1, F2). The facies F3, so-called 'laminite', with abundant radiolarians and a

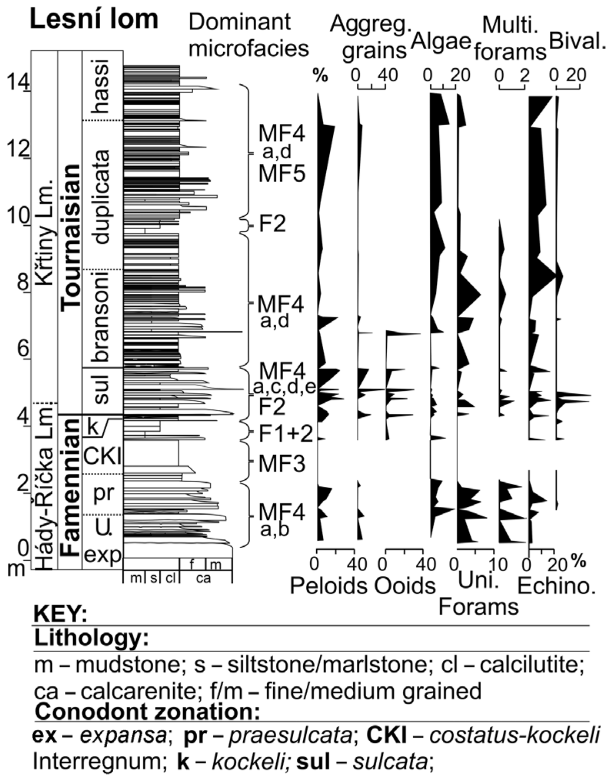

Figure 4. Stratigraphic trends in selected compositional groups (percentages from point counting) in the Lesní lom Quarry section.

distinct bed-parallel lamination, which is emphasized by pressure dissolution and occasional thin laminae of graded calcarenite, probably represents a succession of extremely distal turbidites and a pelagic suspension deposit, presumably modified by bottom currents.

4.c. Facies tracts and compositional variations

Thickening upward trends in the Upper and uppermost Famennian skeletal and peloidal calciturbidites (MF4b and to a lesser extent MF4a) at the Lesní lom section (Fig. 4) are capped by a thick bed of laminite (F3). The overlying siliciclastic horizon comprises mudstones (F1) with lenses of calciturbidites (MF4c, MF4a) and in the upper part, marlstones (F2). The marlstones begin to alternate with peloidal calciturbidites (MF4c) at the very top of the Famennian, where a single level of goniatite-bearing (?*Acutimitoceras* sp.; Kalvoda & Kukal, 1987) wackestone nodules (F5) also occurs. The base of the Tournaisian is marked by the onset of ooidal and skeletal calciturbidites (MF4e, MF4d, MF4c, MF4a) with a distinct drop in the occurrence of algae and multicellular foraminifers (Fig. 4). The heterolithic nature of this interval is expressed by the common alternations of calciturbidites and centimetre-thick marlstones (F2). Within the overlaying Lower Tournaisian mud calciturbidite interval (MF4a prevailing, MF4d and MF5 less common), the second siliciclastic horizon (F2) occurs (Fig. 4).

The Mokrá section is similar to the Lesní lom succession; however, more distal facies prevail (Fig. 3).

https://doi.org/10.1017/S0016756812001057 Published online by Cambridge University Press

Table 1. Facies and microfacies of the studied Moravian Karst sections

Facies code	Grain size/Dunham classification	Bed geometry/bed thickness/bedding and sedimentary structures	Micro-facies code	Allochems dominant/subordinate	Remarks	Interpretation/depositional setting
F1	Lutites/mud to mudstones	Sheet-like, lens-like (~ 0.5 – ~ 10 cm).				Terrigenous suspension deposits.
F2	Siltites/calcareous siltstones to marlstones	Sheet-like (~ 0.5 – ~ 30 cm), massive or slightly laminated.		Bivalves and gastropods in rare laminae.		Suspension deposits.
F3	Calcilutites/lime mudstones with pressure dissolution	Thick bedded (~ 1m), laminated, with rare intercalations of coarser graded laminae with sharp base.	MF3	Radiolarians. Forams and peloids in the rare laminae.	Domains of pure micrite and microsparite are separated by dissolution seams. Rare packstone laminae without intensive dissolution occur.	Distal low-density turbidity current deposits modified by bottom currents + suspension deposits.
F4	Fine-grained calcarenites or calcilutites/wackestones to packstones	Sheet-like (~ 2 – ~ 20 cm), erosive or sharp bases, normal gradation, lamination.	MF4a	Radiolarians, unicellular forams/echinoderms, dasyclad algae, foraminifers, ostracods.	Hydraulic sorting during transport resulting in a fractionation of allochems. Bioturbation is common especially in the upper parts of beds.	Low-density turbidity current deposits. Tb, Td Bouma sequences.
	Fine- to medium-grained calcarenites/packstones to grainstones		MF4b	Peloids, forams, dasyclad algae/ intraclasts, echinoderms, ostracods brachiopods, bryozoa.		Low-density turbidity current deposits. Ta, Tb and Td Bouma sequences.
			MF4c	Echinoderms, dasyclad algae, peloids/forams, ooids, intraclasts, trilobites, bivalves, brachiopods.		
			MF4d	Peloids, dasyclad algae/intraclasts, crinoids, forams, calcisphaerids, bivalves, ostracods, trilobites, ooids, bryozoa.		
			MF4e	Ooids, aggregated grains, peloids, crinoids/dasyclad algae, brachiopods, bivalves, trilobites, bryozoa.		Low-density turbidity current deposits. Ta, Tb Bouma sequences.
F5	Calcisiltites, calcilutites/lime mudstones to wackestones	Lens-like thin-bedded (~ 1 – ~ 10 cm) to sheet-like massive (~ 0.2 – 2 m).	MF5	Radiolarians, sponge spicules, ostracods/bivalves, trilobites, cephalopods.	Bioturbation (burrows are usually filled by coarser allochems or dolomitized). Nodular fabric common.	Suspension deposits (periplatform ooze) well below fair-weather wave base.

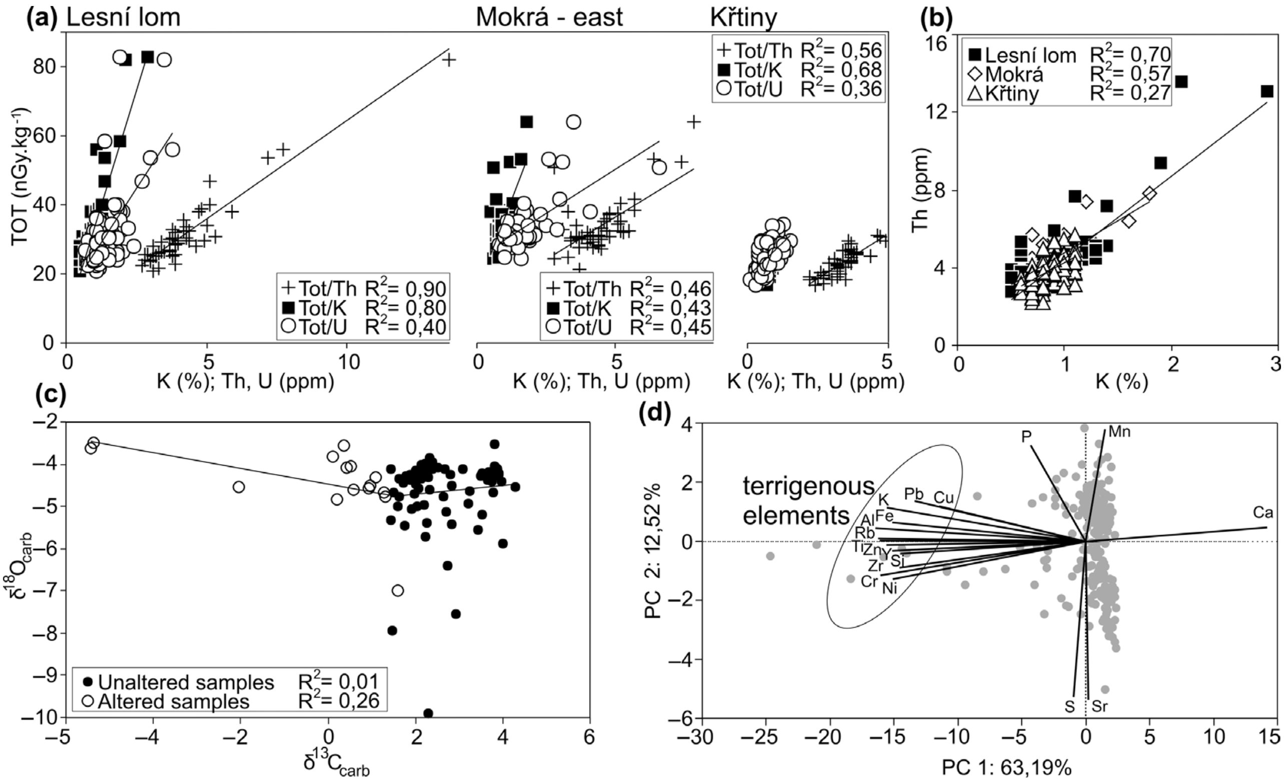

Figure 5. Bivariate plots and linear regression coefficients of the (a) total dose rate (TOT) v. K, U and Th, (b) Th v. K and (c) $\delta^{18}O_{carb}$ v. $\delta^{13}C_{carb}$ from the Moravian Karst sections. (d) Principal component analysis of the EDXRF data from the Moravian Karst.

The Famennian calciturbidite interval consists mainly of the MF4a with occasional thin coarser bases (MF4b). The laminite (F3) is underlain by a black shale layer and overlain by calcareous siltstones with wackestone nodules (MF4a,d) (Fig. 3). Oolitic calciturbidites are absent, and primarily thin-bedded mud calciturbidites (MF4a) predominate in the Lower Tournaisian.

The Křtiny section (Fig. 3) exposes a relatively monotonous succession of nodular wackestones (MF5) with common radiolarians, ostracodes, bivalves and trilobites. Wackestones of the Upper Famennian, pinkish at the base and greyish up section, reveal an upward-thinning trend, which culminates in the strongly nodular interval of the uppermost Famennian. The upward-thickening trend (Fig. 3) with a colour transition from yellow to grey slightly nodular wackestones occurs from the base of the Tournaisian.

4.d. Gamma-ray spectra

Covariance between the dose rate (nGy.kg^{-1}) and K, Th and U concentrations (Fig. 5a) demonstrates that the main contribution to the entire gamma-ray signal is derived from Th, followed by K and U. The K and Th concentrations have good covariance (Fig. 5b), which indicates that these typically terrigenous elements (K is incorporated into the lattice of common clay minerals such as illite and Th is adsorbed on the surface of clay minerals) vary proportionally to one other. Their covariance is presumably driven by the dilution effect of $CaCO_3$, which is consistent with the common interpretation of K and Th in GRS logs as the ‘shale content’ or ‘shaliness’ indicator (Rider, 1999; Ehrenberg & Svana, 2001).

In Lesní lom (Fig. 6), the Upper and uppermost Famennian peloidal-bioclastic calciturbidites (MF4b) are characterized by low CGR values (mean CGR 24.7 API) with minima of CGR (20.3 API) and Th/U (< 2) in the laminite (F3). The GRS signal sharply increases in the uppermost Famennian siliciclastic interval (CGR 87.72 API) and then systematically decreases at the D–C boundary and in the basal Tournaisian heterolithic facies (F2 + F4). Another peak in CGR values (87.72 API) is located within the Lower Tournaisian mud calciturbidites (MF4a, MF4d), being associated with the upper siliciclastic interval (F1, F2).

Trends in the GRS values at the Mokrá section (Fig. 6) are almost identical to those from Lesní lom. The Famennian calciturbidites have low K and Th concentrations and CGR values, with the minimum in the laminite (CGR 20.7 API; < 2 Th/U). The maximum U concentrations occur at this level. The overlying sharp increase of the GRS signal in the siliciclastic horizon is replaced by a decreasing trend in the Lower Tournaisian mud calciturbidites.

At the Křtiny section (Fig. 6), the lowest GRS values (CGR 20.7 API) and a high Th/U ratio (> 7) were measured in the reddish Upper Famennian pelagic calcilutites. The GRS signal increases upwards with the maximum values (CGR 40.35 API) located at the top of the uppermost Famennian greyish, strongly nodular calcilutites. The GRS values decrease in the basal

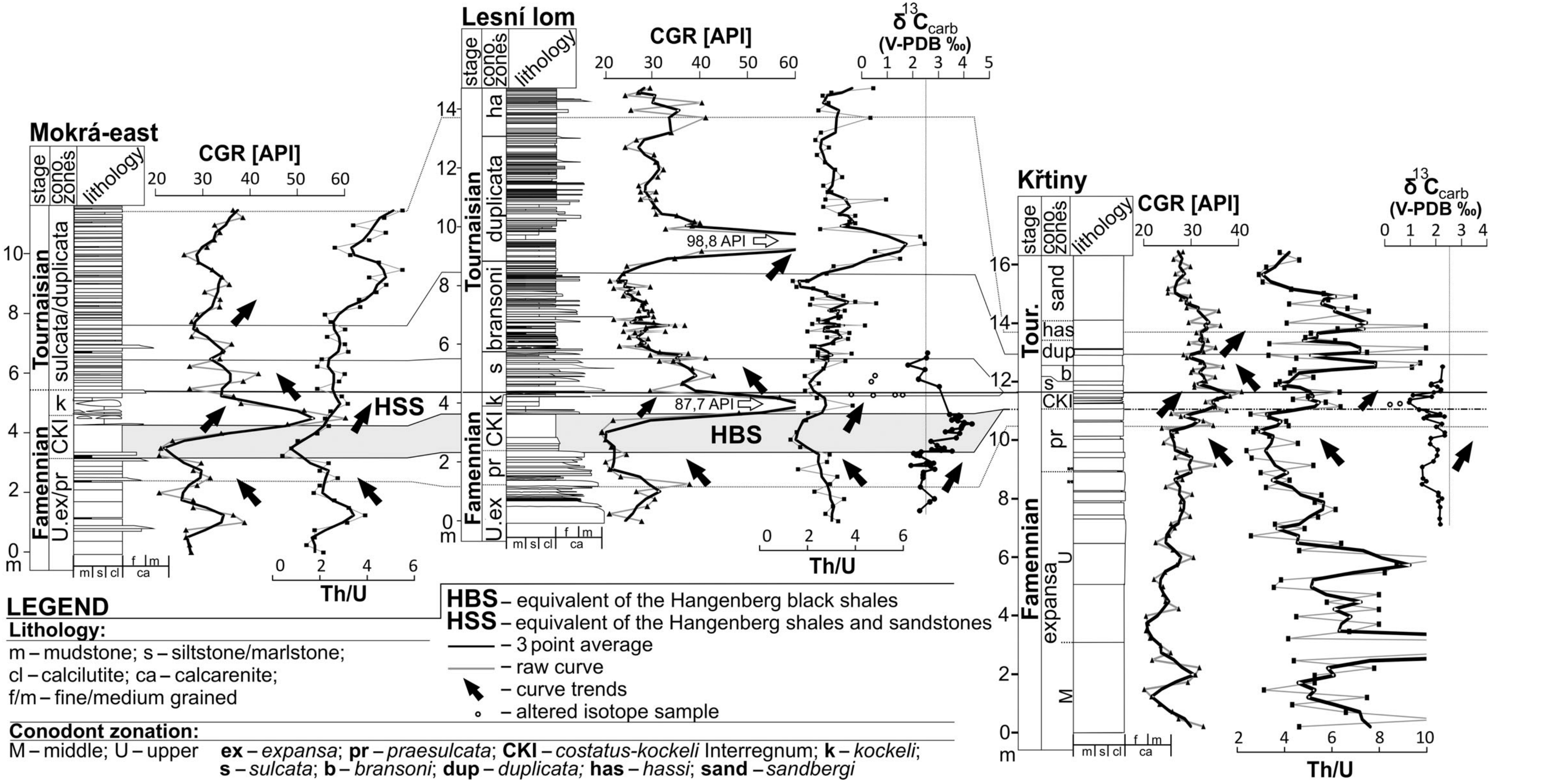

Figure 6. Correlation of the Moravian Karst sections based on biostratigraphy, lithology, spectral gamma-ray logs (CGR and Th/U) and $\delta^{13}C_{carb}$ curves with interpretation of the important stratigraphic horizons.

Tournaisian yellowish calcilutites and then slightly increase again in the Lower Tournaisian.

4.e. Isotope geochemistry

Covariance of $\delta^{13}C_{carb}$ and $\delta^{18}O_{carb}$ in marine carbonates is regarded as evidence of the diagenetic overprint of C isotopes (Rosales, Quaseda & Robles, 2001). The degree of the majority of the measured samples' covariance is low (Fig. 5c); therefore, the isotopic record of the C could be regarded as reflecting the primary signal of the oceanic waters. Only samples with low $\delta^{13}C_{carb}$ have a slight covariance, which reflects diagenetic alteration.

In Lesní lom (Fig. 6), the average $\delta^{13}C_{carb}$ values from the upper Bouma divisions of the calciturbidite beds (MF4a, F5) of the Upper *expansa* and the *praesulcata* zones are ∼ 2.5 ‰ (Fig. 6). A significant positive excursion (∼ 4‰ $\delta^{13}C_{carb}$) is located in the laminite (F3), which belongs to the CKI. The lowest values (∼ 0.5 ‰) were measured in the nodular wackestones (F5) of the *kockeli* Zone. A return to values of ∼ 2.5 ‰ occurs in the samples from the base of the *sulcata* Zone. Certain $\delta^{13}C_{carb}$ values from the *kockeli* Zone and from the base of the *sulcata* Zone are affected by dolomitization and reach distinct negative values (∼ −5‰).

The base of the succession at the Křtiny section (Fig. 6) has uniform $\delta^{13}C_{carb}$ values (∼ 2.1 ‰) in the Upper *expansa* Zone. The values then decrease to ∼ 1.5 ‰ at the end of this Zone and subsequently increase to the background values (∼ 2.5 ‰) in the *praesulcata* Zone. A negative excursion (0.2 ‰) is located within the markedly nodular wackestones of the CKI. The values then increase upwards with small fluctuations throughout the *sulcata* and *bransoni* zones where they reach ∼ 2.2 ‰ $\delta^{13}C_{carb}$.

4.f. Elementary geochemistry

The typically terrigenous elements (Si, Ti, Zr, Rb, Al, etc.) from the studied sections show a strong positive statistical correlation, which is expressed as similar principal component loadings in the principal component analysis (PCA; Fig. 5d), and suggests a common and stable siliciclastic provenance. The strong negative statistical correlation of these elements with Ca (Fig. 5d) indicates that the variability in the terrigenous elements is driven by the effect of 'dilution' by $CaCO_3$. This supports the GRS interpretation. The Mn, Sr and P contents do not correlate with the terrigenous elements (Fig. 5d).

Concentrations of Si, Ti, Zr, Rb, usually normalized to Al (for elimination of the dilution effect), can be used as proxies for relative changes in the sedimentation rates of detrital mineral phases such as quartz (Si), heavy minerals (Ti, Zr) and detrital clays (K) in carbonates (Sageman & Lyons, 2005). Mn and rare earth elements proved useful as palaeoredox proxies (Sageman & Lyons, 2005).

The Upper and uppermost Famennian calciturbidites and the laminite at the Lesní lom section (Fig. 7) are characterized by a low content of terrigenous element concentrations and higher Sr/Al ratios. An increase in the content of the terrigenous elements, with high Zr/Al and a decrease in Sr/Al and Mn/Al ratios, takes place in the siliciclastic interval just below the D–C boundary. The Lower Tournaisian heterolithic interval with mud calciturbidites has a fluctuating content of terrigenous elements, low and stable Zr/Al and lower Sr/Al and Mn/Al ratios (Fig. 7). In Mokrá the laminite is characterized, as is the case in Lesní lom, by a growing Mn/Al and Sr/Al (Fig. 7). A decrease in these values takes place in the siliciclastic interval while the Al content increases. The Křtiny section is characterized by low contents of terrigenous elements in the Upper and uppermost Famennian wackestones, and their subsequent pronounced increase (with higher Zr/Al) just below the D–C boundary where the Sr/Al ratio concomitantly decreases (Fig. 7).

5. Discussion

5.a. Biostratigraphic correlation

The study of the Moravian D–C sections reveals numerous problems associated with the application of conodont biostratigraphy in the D–C boundary definition (Kaiser *et al.* 2006). First, owing to the rare occurrence of the early siphonodellids in the Famennian, the base of the *praesulcata* Zone cannot be fixed precisely (Fig. 3). Second, the recognition of the standard Middle *praesulcata* Zone of Ziegler & Sandberg (1984), which is defined by the last occurrence of *Palmatolepis gracilis gonioclymeniae*, is problematic owing to the absence of this index in the uppermost Famennian of the Moravian Karst (Fig. 3). A possible solution is the application of the alternative zonation of Ji (1985) and Kaiser *et al.* (2009), who proposed the CKI, which represents the main extinction interval of the Hangenberg Event (Kaiser *et al.* 2009). The main biostratigraphic problem, however, is connected with the supposed *Si. praesulcata – Si. sulcata* evolutional lineage (Feist & Flajs, 1988). In the Moravian Karst sections (Lesní lom and Křtiny), the FAD of *Si. sulcata* was recorded in the *praesulcata* Zone, just before the entry of the *Si. praesulcata* and protognathodid fauna (Fig. 3). This is in accordance with data from Franconia (Germany), where *Siphonodella sulcata* morphotypes enter below the Hangenberg Event almost simultaneously with the entry of *Si. praesulcata* (Tragelehn, 2010). The biostratigraphically valuable protognathodid fauna is relatively abundant in Lesní lom, where the FAD of the early *Protognathodus* species corresponds with their known global range (Fig. 3). It is a scarce feature in the majority of the global scenario (Corradini *et al.* 2011). In Křtiny, on the other hand, the protognathodid fauna is missing and, therefore, the *kockeli* Zone cannot be recognized, most probably due to the hiatus (Fig. 3). This

https://doi.org/10.1017/S0016756812001057 Published online by Cambridge University Press

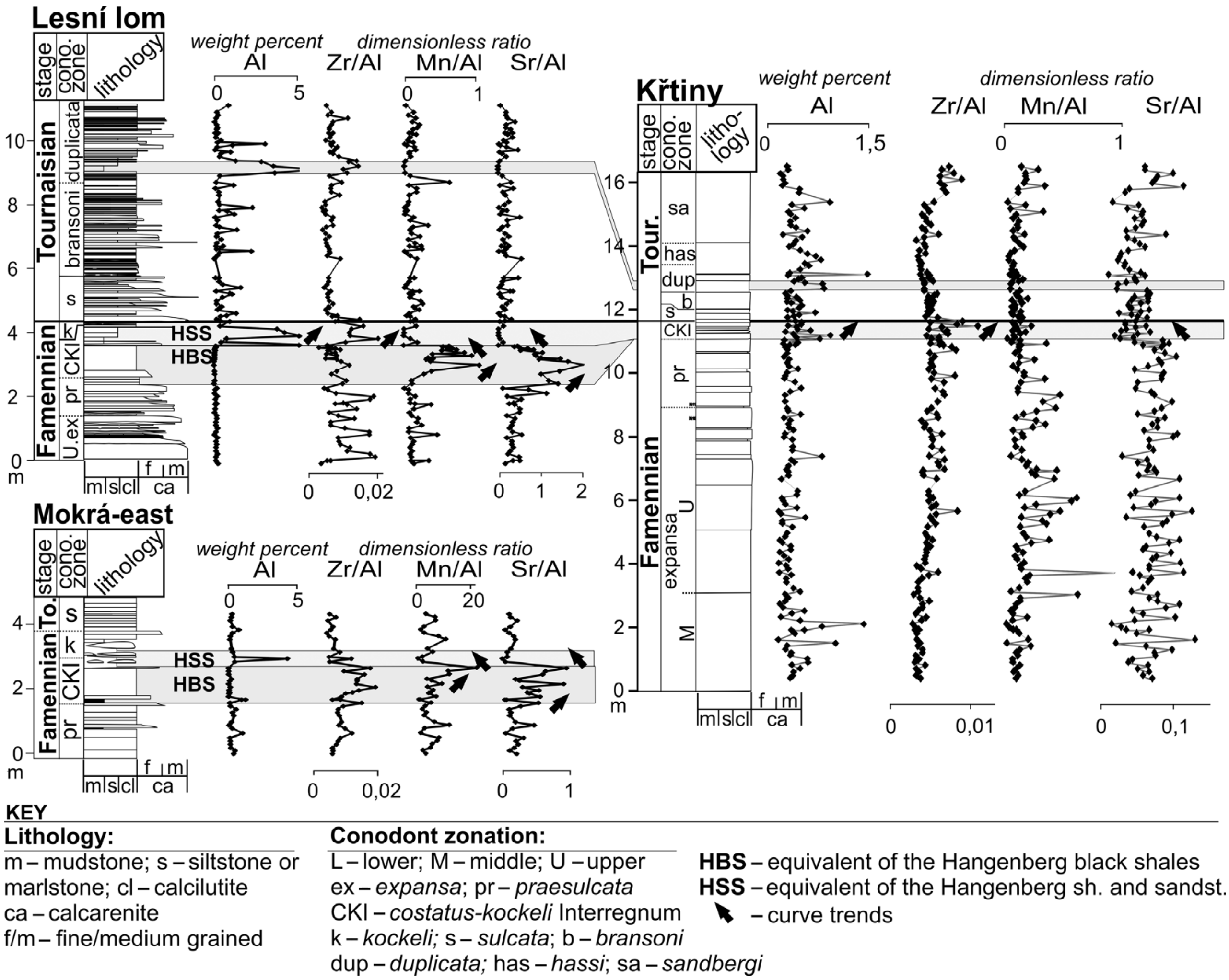

Figure 7. Correlation based on the chosen geochemical proxies of the Moravian Karst sections.

stratigraphic gap also comprises the lower part of the *sulcata* Zone (Fig. 6). It is supported by the abrupt appearance of the transitional morphotypes *Si. sulcata – Si. bransoni* just above the D–C boundary.

In terms of foraminiferal zonation, the entry of *Tournayellina beata pseudobeata* recognized in Belgium (Poty, Devuyst & Hance, 2006), the Urals (Reitlinger & Kulagina, 1987; Pazukhin, Kulagina & Sedaeva, 2009) and China (Hance *et al.* 2011) represents an important event. In contrast to the other sections, the Moravian sections enable the precise establishment of its FAD to the higher part of the CKI (Fig. 3). A multidisciplinary approach to the study of the entry of *T. beata pseudobeata* in the Belgian sections is underway.

5.b. Regional correlation between the Moravian Karst and the Carnic Alps

The observed geochemical and petrophysical patterns can be correlated between sections from two different deep-water carbonate depositional environments of the Moravian Karst (Figs 6, 7). The main correlatable pattern is the low GRS signal due to low terrigenous element content in the Upper and uppermost Famennian (the Upper *expansa* and *praesulcata* zones and the lower part of the CKI) and the subsequent sharp increase in GRS values and terrigenous elements just below the D–C boundary (within the CKI). The decrease in GRS values together with the terrigenous content upwards through the basal Tournaisian and the second increase in the Lower Tournaisian *duplicata* Zone are also good correlatable patterns.

The laminite horizon at the base of the CKI with the weak GRS signal and the positive $\delta^{13}C_{carb}$ excursion in Lesní lom is absent at the Křtiny section (Fig. 6). A possible explanation is provided by the stratigraphic gap, which encompasses the peak $\delta^{13}C_{carb}$ interval. The stratigraphic gap in Křtiny is also supported by the absence of the high Mn/Al ratio, which was observed at this level in Lesní lom and Mokrá (Fig. 7). A decrease of $\delta^{13}C$ (Fig. 6) and Sr/Al (Fig. 6) just below the D–C boundary, coinciding with the high GRS values (Fig. 6) and Zr/Al ratio, was documented both in the Lesní lom and Křtiny sections (Fig. 7).

The petrophysical and geochemical trends from the Moravian Karst can be well correlated with the multiproxy dataset from the Grüne Schneid section of the Carnic Alps, Austria (Figs 1, 8). The positive $\delta^{13}C_{carb}$ excursion in the CKI and the *kockeli* Zone at the Grüne Schneid section (Kaiser *et al.* 2006) correlates with a similar $\delta^{13}C_{carb}$ peak at the Trolp section (Graz Palaeozoic, Austria) and $\delta^{13}C_{org}$ at the Hasselbachtal section (Rheinische Schiefergebirge, Germany) (Kaiser *et al.* 2006; Kaiser, Steuber & Becker, 2008). This isotope peak correlates with the positive $\delta^{13}C_{carb}$ excursion exactly at the same stratigraphic level (CKI) in Lesní lom and coincides with the low GRS values, low concentrations of terrigenous elements and increasing Mn/Al and Sr/Al at both the Grüne Schneid and Lesní lom sections (Fig. 8). Just above the isotopic shift, the GRS signal and the contents of the terrigenous elements significantly increase and Mn/Al with Sr/Al decrease both in the Lesní lom (CKI) and the Grüne Schneid sections (the *kockeli* Zone). The high GRS values decrease from the base of the *sulcata* Zone at both sections (Fig. 8).

5.c. Equivalents of the Hangenberg black shales

The Upper and uppermost Famennian succession in Lesní lom and Mokrá comprise calciturbidites with common algae, peloids, foraminifers and crinoids (Fig. 4) representing the mixed autotroph-heterotroph carbonate factory (T factory; Schlager, 2005). The overlying laminite horizon with the abundance of planktonic radiolarians and the millimetre-thick calciturbidites and bottom-current deposits in the lower part of the CKI is assumed to have recorded initial deceleration of carbonate production, having manifested itself by reduced allochem shedding into the deep basin. This almost siliciclastic-free horizon is characterized by a positive $\delta^{13}C_{carb}$ excursion at Lesní lom (Fig. 6). Enhanced burial of organic matter has led to the black shale deposition in some regions (Hangenberg black shales and their equivalents, e.g. Exshaw shales) and thus to a depletion of the isotopically lighter organic carbon from the global oceanic reservoir (Caplan & Bustin, 1999; Kaiser *et al.* 2006; Kaiser, Steuber & Becker, 2008). The resulting positive Hangenberg Event $\delta^{13}C_{carb}$ excursion was thus documented at sections where the black shales are absent and carbonates were preserved, e.g. at the Grüne Schneid, Carnic Alps (Kaiser *et al.* 2006), Trolp, Graz Palaeozoic (Kaiser, Steuber & Becker, 2008), Glen Wood Canyon, Colorado (Myrow *et al.* 2011) and Lesní lom, Moravian Karst (presented herein). The enhanced carbon burial could have been connected with the oceanic mixing, when the cold, nutrient-rich upwelling waters (Caplan & Bustin, 1999) reached the shelves and carbonate platforms, where an increase in bioproductivity and consequent eutrophication was produced (Caplan, Bustin & Grimm, 1996). The upwelled cool waters undersaturated with respect to calcium carbonate might have caused dissolution of the pelagic, slowly sedimented, slope carbonates (Bandel, 1974) and produced the stratigraphic gap in the Křtiny section. The subsequent onset of dysoxic conditions, caused by high oxygen utilization in the bottom waters, is regarded as the Hangenberg Event *sensu stricto* connected with the mass extinction (Kaiser *et al.* 2009). The relative O_2 depletion trend can be inferred from the decreasing curve of the Th/U (Adams & Weaver, 1958) also in the Moravian Karst and Carnic Alps (Figs 6, 8). In contrast, an interesting feature of the HBS-equivalent interval at Lesní lom, Mokrá and Grüne Schneid is the increasing Mn/Al ratio, which is usually used as the proxy for growing oxygenation (Sageman & Lyons, 2005; Roy, 2006). This contradiction could be explained by the precipitation of Mn oxyhydroxides in the halocline (the zone of the 'bathub ring'; Maynard, 2005) where it reached the upwelled water mass. The considerable amount of Mn precipitates were consequently buried in a reducing zone below ('manganese pump') where dissolution provides adequate Mn^{2+} and the reaction with dissolved bicarbonate forms Mn carbonates (Roy, 2006). A slight increase in the Sr/Al ratio in all investigated sections is evidence for the low sedimentation rate in this stratigraphic level. An origin of higher Mn and Sr content from the continental runoff is unlikely because the discussed HBS-equivalent level is almost free of terrigenous elements and therefore the source could be in the upwelled deep waters.

5.d. Equivalents of the Hangenberg shales and sandstones

The short but significant lithological change from the carbonates to the fine siliciclastic sediments just above the laminite at Lesní lom and Mokrá (Fig. 6) and thin-bedded nodular wackestones at Křtiny (Fig. 6) and Grüne Schneid (Fig. 8) records a carbonate crisis and enhanced continental input of siliciclastic sediments. The high Zr/Al ratio at Lesní lom is interpreted as the coarsening of the terrigenous siliciclastic input. This horizon is thus correlated with the lowstand HSS facies and with their equivalents (Van Steenwinkel, 1993). The high content of ooids and peloids in the interval of the upper CKI to the *bransoni* Zone (Fig. 4) can be interpreted as products of distally steepened ramp sedimentation (Read, 1982) after the emersion of carbonate platforms (Kalvoda, 1982). According to Wright (1994), the extensive development of oolite shoals is a distinctive feature of early Carboniferous carbonate systems when extensive upwelling currents moved cool, nutrient-rich waters into the shallow seas creating conditions suitable for extensive inorganic carbonate precipitation.

5.e. Interpretation of the relative sea-level changes

The upwelling currents and HBS deposition were probably associated with the transgressive to highstand system tract (maximum flooding surface), as is evidenced by landward facies shifts (e.g. Van Steenwinkel, 1993). It is also evidenced from Lesní lom and Mokrá by the onset of the relatively deeper water facies of laminite (F3; Table 1; Fig. 4) with respect to the underlying skeletal calciturbidites (F4; Table 1; Fig. 4). The enhanced continental input of coarser terrigenous material above the $\delta^{13}C_{carb}$ excursion (Figs 6–8) was

https://doi.org/10.1017/S0016756812001057 Published online by Cambridge University Press

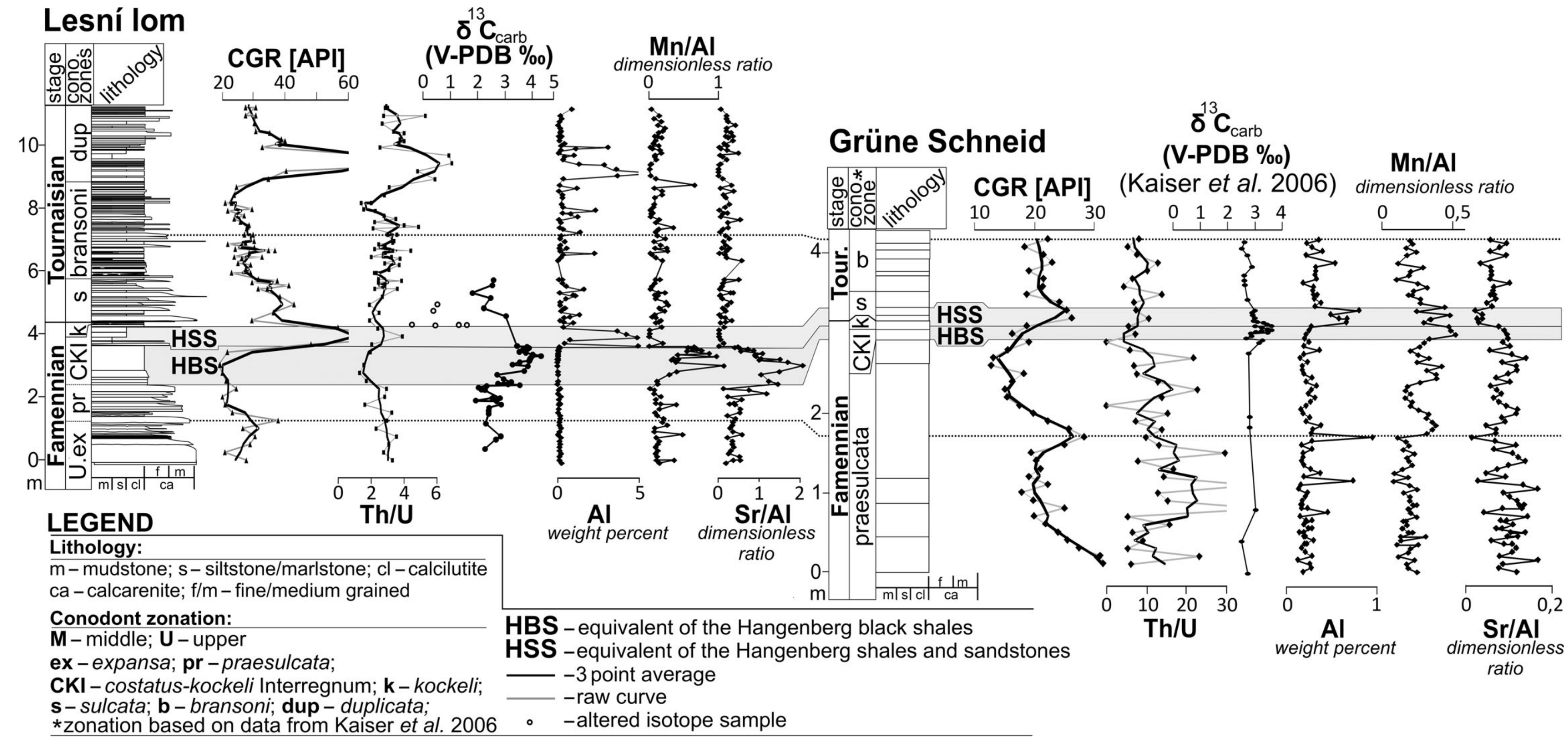

Figure 8. Correlation based on the gamma-ray logs, $\delta^{13}C_{carb}$ and element geochemical proxies between the Moravian Karst (represented by the Lesní lom Quarry) and the Carnic Alps (Grüne Schneid) with an interpretation of the main correlative horizons.

probably connected with the glacioeustatic sea-level fall (Isaacson *et al*. 1999, 2008) and the demise of the carbonate platform (Kalvoda, 1982).

In summary, as the petrophysical and geochemical proxies largely reflect the global glacioeustatic oscillations, their time resolution is beyond the scope of biostratigraphy. The conodont zonation is facing serious problems at the D–C boundary connected both with the problematic taxonomy and the scarcity of first siphonodellids and discontinuous occurrences of protognathodids (Corradini *et al*. 2011; Kaiser & Corradini, 2011). The positive $\delta^{13}C_{carb}$ excursion of the Hangenberg Event recognized both in Eurasia and North America (Brand, Legrand-Blain & Streel, 2004; Buggisch & Joachimski, 2006; Kaiser *et al*. 2006; Kaiser, Steuber & Becker, 2008; Cramer *et al*. 2011; Myrow *et al*. 2011) of less than 100 000 years duration (Davydov, Schmitz & Korn, 2011) represents a useful tool for chronostratigraphic correlations which can contribute to the calibration of the conodont zonation. The GRS trends and higher Sr/Al and Mn/Al ratios both in the Carnic Alps and Moravia correlate well with the $\delta^{13}C_{carb}$ excursion (Fig. 8). They thus represent additional perspective proxies for the recognition of the glacioeustatic oscillations at the D–C boundary and calibration of biostratigraphy, the study of which should also be extended to other sections.

6. Conclusions

Petrophysical and geochemical changes across the D–C boundary in the Moravian Karst and Carnic Alps sections provide a useful proxy for the determination of the Hangenberg Black Shales Event (HBE *sensu stricto*; Fig. 8) and good support for its interpreted origin due to oceanic upwelling, eutrophication and glacioeustatic oscillations. While the positive $\delta^{13}C_{carb}$ anomaly of the Hangenberg Event has already been identified worldwide, previously unknown peaks in GRS, terrigenous elements and Mn/Al (Fig. 8) represent new possible proxies for the calibration of the biostratigraphy at the D–C boundary. The correlative potential of these proxies is high and capable of refining the biostratigraphic division of the D–C boundary interval. The obtained results support the views of Walliser (1984) who regarded the Hangenberg Event as worldwide, synchronous and a natural D–C boundary. Consequently, the new biostratigraphical definition of the D–C boundary that is under discussion should approach this event.

Acknowledgements. This research has been financially supported by the Czech Science Foundation (grant number P210/11/1891). The first author is a Brno Ph.D. Talent Scholarship Holder, funded by the Brno City Municipality.

References

Adams, J. A. S. & Weaver, C. E. 1958. Thorium-to-uranium ratios as indicators of sedimentary processes; example of concept of geochemical facies. *American Association of Petroleum Geologists Bulletin* **42**, 387–430.

Bábek, O. & Kalvoda, J. 2001. Compositional variations and patterns of conodont reworking in Late Devonian and Early Carboniferous calciturbidites (Moravia, Czech Republic). *Facies* **44**, 211–26.

Bábek, O., Kalvoda, J., Aretz, M., Cossey, P. J., Devuyst, F. X., Herbig, H. G. & Sevastopulo, G. D. 2010. The correlation potential of magnetic susceptibility and outcrop gamma-ray logs at Tournaisian-Visean boundary sections in Western Europe. *Geologica Belgica* **13**, 291–308.

Bandel, K. 1974. Deep-water limestones from the Devonian-Carboniferous of the Carnic Alps, Austria. In *Pelagic Sediments: On Land and Under the Sea* (eds K. J. Hsü & H. C. Jenkyns), pp. 71–92. Special Publication of the International Association of Sedimentologists 1.

Barskov, I. S., Simakov, K. V., Alekseev, A. S., Bogoslovsky, B. I., Byvsheva, T. V., Gaciev, M. H., Kononova, L. N., Kochetkova, N. M., Kusina, L. F. & Reitlinger, E. A.1984. Devonian-Carboniferous transitional deposits of the Berchogur section, Mugodzhary, USSR (Preliminary report). *Courier Forschungsinstitut Senckenberg* **67**, 207–30.

Boardman, M. R. & Neumann, A. C. 1984. Sources of periplatform carbonates: Northwest Providence Channel, Bahamas. *Journal of Sedimentary Petrology* **54**, 1110–23.

Brand, U., Legrand-Blain, M. & Streel, M. 2004. Biochemostratigraphy of the Devonian-Carboniferous boundary global stratotype section and point, Griotte Formation, La Serre, Montagne Noire, France. *Palaeogeography, Palaeoclimatology, Palaeoecology* **205**, 337–57.

Buggisch, W. & Joachimski, M. M. 2006. Carbon isotope stratigraphy of the Devonian of central and southern Europe. *Palaeogeography, Palaeoclimatology, Palaeoecology* **240**, 66–88.

Caplan, M. L. & Bustin, R. M. 1999. Devonian-Carboniferous Hangenberg mass extinction event, widespread organic-rich mudrock and anoxia: causes and consequences. *Palaeogeography, Palaeoclimatology, Palaeoecology* **148**, 187–207.

Caplan, M. L., Bustin, R. M. & Grimm, K. A. 1996. Demise of a Devonian-Carboniferous carbonate ramp by eutrophication. *Geology* **24**, 715–18.

Caputo, M. V. & Crowell, J. C. 1985. Migration of glacial centers across Gondwana during Paleozoic Era. *Geological Society of America Bulletin* **96**, 1020–36.

Corradini, C., Kaiser, S. I., Perri, M. C. & Spalleta, C. 2011. *Protognathodus* (Conodonta) and its potential as a tool for defining the Devonian/Carboniferous boundary. *Rivista Italiana di Paleontologia e Stratigrafia* **117** (1), 15–28.

Cramer, B. D., Day, J. E., Saltzman, M. R. & Witzke, B. J. 2011. The uppermost Famennian Hangenberg excursion in North America and search for the base of the Carboniferous. *Geological Society of America, Abstracts with Programs* **43** (1), 151.

Davydov, V., Schmitz, M. & Korn, D. 2011. The Hangenberg Event was abrupt and short at the global scale: the quantitative integration and intercalibration of biotic and geochronologic data within the Devonian-Carboniferous transition. *Geological Society of America, Abstracts with Programs* **43** (5), 128.

Ehrenberg, S. N. & Svana, T. A. 2001. Use of spectral gamma-ray signature to interpret stratigraphic surfaces in carbonate strata; an example from the Finnmark carbonate platform (Carboniferous-Permian), Barents Sea. *American Association of Petroleum Geologists Bulletin* **85**, 295–308.

FLAJS, G. & FEIST, R. 1988. Index conodonts, trilobites and environment of the Devonian-Carboniferous boundary beds at La Serre (Montagne Noire, France). *Courier Forschungsinstitut Senckenberg* **100**, 53–107.

HALGEDAH, S. L., JARRARD, R. D., BRETT, C. E. & ALLISON, P. A. 2009. Geophysical and geological signatures of relative sea level change in the upper Wheeler Formation, Drum Mountains, West-Central Utah: a perspective into exceptional preservation of fossils. *Palaeogeography, Palaeoclimatology, Palaeoecology* **277**, 34–56.

HANCE, L., HOU, H., VACHARD, D., DEVUYST, F. X., KALVODA, J., POTY, E. & WU, X. 2011. *Upper Famennian to Visean Foraminifers and Some Carbonate Microproblematica From South China – Hunan, Guangxi and Guizhou*. Beijing: Beijing Geological Publishing House, 359 pp.

HLADIL, J. 1994. Moravian Middle and Late Devonian buildups: evolution in time and space with respect to Laurussian shelf. *Courier Forschungsinstitut Senckenberg* **172**, 111–25.

ISAACSON, P. E., HLADIL, J., SHEN, J. W., KALVODA, J. & GRADER, G. 1999. Late Devonian (Famennian) glaciation in South America and marine offlap on other continents. *Abhandlungen der Geologischen Bundesanstalt* **54**, 239–57.

ISAACSON, P., DÍAZ-MARTÍNEZ, E., GRADER, G. W., KALVODA, J., BÁBEK, O. & DEVUYST, F. X. 2008. Late Devonian–earliest Mississippian glaciation in Gondwanaland and its biogeographic consequences. *Palaeogeography, Palaeoclimatology, Palaeoecology* **268**, 126–42.

JI, Q. 1985. Study on the phylogeny, taxonomy, zonation and biofacies of *Siphonodella* (conodonta). *Institute of Geology, Bulletin* **11**, 51–75.

KAISER, S. I. 2009. The Devonian/Carboniferous stratotype section La Serre (Montagne Noire) revisited. *Newsletters on Stratigraphy* **43** (2), 195–205.

KAISER, S. I., BECKER, R. T., SPALLETTA, C. & STEUBER, T. 2009. High-resolution conodont stratigraphy, biofacies and extinctions around the Hangenberg Event in pelagic successions from Austria, Italy and France. *Palaeontographica Americana* **63**, 97–139.

KAISER, S. I. & CORRADINI, C. 2011. The early siphonodellids (Conodonta, Late Devonian-Early Carboniferous): overview and taxonomic state. *Neues Jahrbuch für Geologie und Paläontologie, Abhandlungen* **261**, 19–35.

KAISER, S. I., STEUBER, T. & BECKER, T. R. 2008. Environmental change during the Late Famennian and Early Tournaisian (Late Devonian–Early Carboniferous): implications from stable isotopes and conodont biofacies in southern Europe. *Geological Journal* **43**, 241–60.

KAISER, S. I., STEUBER, T., BECKER, T. R. & JOACHIMSKI, M. M. 2006. Geochemical evidence for major environmental change at the Devonian–Carboniferous boundary in the Carnic Alps and the Rhenish Massif. *Palaeogeography, Palaeoclimatology, Palaeoecology* **240**, 146–60.

KALVODA, J. 1982. Biostratigraphy and palaeobiogeography of the Famennian and Lower Carboniferous in southeastern and eastern Moravia. *Zemní Plyn Nafta* **26** (4) 571–84.

KALVODA, J. 1986. Upper Frasnian-Lower Tournaisian events and evolution of calcareous foraminifera, close links to climatic changes. In *Global Bio-Events: A Critical Approach: Proceedings of the First International Meeting of the IGCP Project 216, "Global Biological Events in Earth History"* (ed. O. H. Walliser), pp. 225–36. Lecture Notes in Earth Sciences, 8. Berlin, Heidelberg: Spring-Verlag.

KALVODA, J. 1998. The main phases of extension in the eastern part of the Rhenohercynian Zone. *Acta Universitatis Carolinae, Geologica* **42**, 274–5.

KALVODA, J. 2002. Late Devonian – Early Carboniferous foraminiferal fauna: zonation, evolutionary events, paleobiogeography and tectonic implications. *Folia* **39**, 213 pp.

KALVODA, J., BÁBEK, O., FATKA, O., LEICHMANN, J., MELICHAR, R. & ŠPAČEK, P. 2008. Brunovistulian terrane (Bohemian Massif, Central Europe) from late Proterozoic to late Paleozoic: a review. *International Journal of Earth Sciences* **97**, 497–517.

KOPTÍKOVÁ, L., BÁBEK, O., HLADIL, J. & SLAVÍK, L. 2010. Stratigraphic significance and resolution of spectral reflectance logs in Lower Devonian carbonates of the Barrandian area, Czech Republic; a correlation with magnetic susceptibility and gamma-ray logs. *Sedimentary Geology* **225**, 83–98.

KALVODA, J., BÁBEK, O. & MALOVANÁ, A. 1999. Sedimentary and biofacies record in calciturbidites at the Devonian-Carboniferous boundary in Moravia (Moravian-Silezian Zone, Middle Europe). *Facies* **41**, 141–58.

KALVODA, J. & KUKAL, Z. 1987. Devonian-Carboniferous boundary in the Moravian Karst at Lesní lom, Brno – Líšeň, Czechoslovakia. *Courier Forschungsinstitut Senckenberg* **98**, 95–117.

KALVODA, J., LEICHMANN, J., BÁBEK, O. & MELICHAR, R. 2003. Brunovistulian Terrane (Central Europe) and Istanbul Zone (NW Turkey): Late Proterozoic and Paleozoic tectonostratigraphic development and paleogeography. *Geologica Carpathica* **54**, 139–52.

KALVODA, J., MELICHAR, R., BÁBEK, O. & LEICHMANN, J. 2002. Late Proterozoic-Paleozoic tectonostratigraphic development and paleogeography of Brunovistulian Terrane and comparison with other terranes at the SE margin of Baltica-Laurussia. *Journal of the Czech Geological Society* **47**, 81–102.

KULAGINA, E. I., GIBSHMAN, N. B. & PAZUKHIN, V. N. 2003. Foraminiferal zonal standard for the Lower Carboniferous of Russia and its correlation with conodont zonation. *Rivista Italiana di Paleontologia e Stratigrafia* **109** (2), 173–85.

LÜNING, S., WENDT, J., BELKA, Z. & KAUFMANN, B. 2004. Temporal-spatial reconstruction of the early Frasnian (Late Devonian) anoxia in NW Africa; new field data from the Ahnet Basin (Algeria). *Sedimentary Geology* **163**, 237–64.

MAYNARD, J. B. 2005. Manganiferous sediments, rocks, and ores. In *Sediments, Diagenesis, and Sedimentary Rocks: Treatise on Geochemistry* 7 (ed. F. T. Mackenzie), pp. 289–308. Amsterdam: Elsevier.

MYROW, P. M., STRAUSS, J. V., CREVELING, J. R., SICARD, K. R., RIPPERDAN, R., SANDBERG, CH. A. & HARTENFELS, S. 2011. A carbon isotopic and sedimentological record of the latest Devonian (Famennian) from the Western U.S. and Germany. *Palaeogeography, Palaeoclimatology, Palaeoecology* **306**, 147–59.

PAZUKHIN, V. N., KULAGINA, E. I. & SEDAEVA, K. M. 2009. The Devonian/Carboniferous boundary on the western slope of the South Urals. In *Carboniferous Type Sections in Russia and Potential Global Stratotypes: Southern*

Urals Session. Proceedings of the International Field Meeting 'The historical type sections, proposed and potential GSSP of the Carboniferous in Russia' (Ufa-Sibai, August 13–18, 2009) (eds V. N. Puchkov, E. I. Kulagina, S. V. Nikolaeva & N. N. Kochetova), pp. 22–33. [in Russian].

POSTMA, G. & TEN VEEN, J. H. 1999. Astronomically and tectonically linked variations in gamma-ray intensity in Late Miocene hemipelagic successions of the Eastern Mediterranean Basin. *Sedimentary Geology* **128**, 1–12.

POTY, E., DEVUYST, F. X. & HANCE, L. 2006. Upper Devonian and Mississippian foraminiferal and rugose coral zonations of Belgium and Northern France: a tool for Eurasian correlations. *Geological Magazine* **143**, 829–57.

READ, J. F. 1982. Carbonate platforms on passive (extensional) continental margins: types, characteristics, and evolution. *Tectonophysics* **81**, 195–212.

REITLINGER, E. A. & KULAGINA, E. I. 1987. Foraminifera. In *Fauna i Biostratigrafiya Pogranichnykh Otlozheniy Devona i Karbona Berchogura (Mugodzhary)* (ed. V. I. Maslov), pp. 68–75. Moscow: Nauka Press.

RIDER, M. H. 1999. *The Geological Interpretation of Well Logs*. Whittles Publishing Services, 288 pp.

ROSALES, I., QUASEDA, S. & ROBLES, S. 2001. Primary and diagenetic isotopic signals in fossils and hemipelagic carbonates: the Lower Jurassic of northern Spain. *Sedimentology* **48**, 1149–69.

ROY, S. 2006. Sedimentary manganese metallogenesis in response to the evolution of the Earth system. *Earth-Science Reviews* **77**, 273–305.

SAGEMAN, B. B. & LYONS, T. W. 2005. Geochemistry of fine-grained sediments and sedimentary rocks. In *Sediments, Diagenesis, and Sedimentary Rocks: Treatise on Geochemistry* 7 (ed. F. T. Mackenzie), pp. 115–58. Amsterdam: Elsevier.

SANDBERG, C. A., ZIEGLER, W., LEUTERITZ, K. & BRILL, S. M. 1978. Phylogeny, speciation, and zonation of Siphonodella (Conodonta, Upper Devonian and Lower Carboniferous). *Newsletter on Stratigraphy* **7**, 102–20.

SCHLAGER, W. 2005. *Carbonate Sedimentology and Sequence Stratigraphy*. SEPM Concepts in Sedimentology and Paleontology 8, 200 pp.

STREEL, M., CAPUTO, M. V., LOBOZIAK, S. & MELO, J. H. G. 2000. Late Frasnian-Famennian climates based on palynomorph analyses and the question of the Late Devonian glaciations. *Earth-Science Reviews* **52**, 121–73.

SVENDSEN, J. B. & HARTLEY, N. R. 2001. Comparison between outcrop spectral gamma ray logging and whole rock geochemistry: implications for quantitative reservoir characterisation in continental sequences. *Journal of Marine and Petroleum Geology* **18**, 657–70.

TRAGELEHN, H. 2010. Short note on the origin of the conodont genus Siphonodella in the Uppermost Famennian. *Subcommission on Devonian Stratigraphy, Newsletter* **23**, 41–3.

VACHARD, D., PILLE, L. & GAILLOT, J. 2010. Palaeozoic foraminifera: systematics, palaeoecology and response to global changes. *Revue de Micropaléontologie* **53**, 209–54.

VAN STEENWINKEL, M. 1993. The D/C boundary: comparison between the Dinant synclinorium and the northern border of the Rhenish Slate Mountains, a sequence-stratigraphic view. *Annales de la Société Géologique de Belgique* **115** (2), 665–81.

VEIZER, J. 2009. Carbon isotope variations over geologic time. In *Encyclopedia of Paleoclimatology and Ancient Environments* (ed. V. Gornitz), pp. 128–33. Dordrecht: Springer.

WALLISER, O. H. 1984. Pleading for a natural D/C boundary. *Courier Forschungsinstitut Senckenberg* **67**, 241–6.

WRIGHT, V. P. 1994. Early Carboniferous carbonate systems: an alternative to the Cainozoic paradigm. *Sedimentary Geology* **93**, 1–5.

ZIEGLER, W. & SANDBERG, C. A. 1984. Palmatolepis-based revision of upper part of standard Late Devonian conodont zonation. In *Conodont Biofacies and Provincialism* (ed. D. L. Clark), pp. 179–94. Geological Society of America, Special Paper no. 196.